Theoretical and Applied Fracture Mechanics 92 (2017) 289–297

Contents lists available at ScienceDirect

Theoretical and Applied Fracture Mechanics

journal homepage: www.elsevier.com/locate/tafmec

Residual stresses in condition monitoring and repair of thermal power generation components

M.N. James [a,b,*], D.G. Hattingh [b], D. Asquith [c], M. Newby [d], P. Doubell [d]

[a] School of Engineering, University of Plymouth, Plymouth, England, United Kingdom
[b] Mechanical Engineering, Nelson Mandela Metropolitan University, Port Elizabeth, South Africa
[c] Engineering and Mathematics, Sheffield Hallam University, Sheffield, England, United Kingdom
[d] Eskom Holdings SOC Ltd, Rosherville, Johannesburg, South Africa

ARTICLE INFO

Article history:
Received 27 January 2017
Accepted 10 March 2017
Available online 12 March 2017

Keywords:
Residual stresses
Thermal power generation
Turbine blade and disc
Friction taper hydro-pillar processing
Weld repair
Cracking
System of systems

ABSTRACT

Residual stresses have a significant impact on fatigue and fracture of engineering components and structures, with an effect that is largely dependent on the sign of the residual stress relative to that of the applied stress, i.e. on whether they add to, or subtract from, the applied stress. The present paper will emphasise the importance of detailed knowledge of residual stresses to applications in thermal power generation. The context of the examples is condition monitoring and repair procedures where assessment of the influence of residual stress fields is important to both fatigue and fracture performance, and to certification of the repair procedure itself. The main conclusion in the paper is that the innovative use of solid-state friction taper hydro-pillar processes can offer additional capability in condition monitoring of through-thickness creep damage in thermal power plant, as well as provide cost-effective local repair of creep or fatigue damage in, for example, thick-walled steam pipe and blade-disc attachment holes.

1. Introduction

Residual stresses have a significant impact on the fatigue and fracture performance of engineering components and structures. Their effect can be either positive (life enhancing) or negative (life reducing) and this is largely dependent on whether the residual stress adds to, or subtracts from, the applied stress. Several useful reviews of residual stress and their effects are given in Refs. [1–3]. It is also the case that the high level of residual stress induced during most manufacturing operations may be overlooked by engineering designers (see for example, data on the residual stress level induced during hot [4] and cold [5] rolling). Surface modification techniques and welding are particularly influential in determining fatigue and fracture performance and, in the case of welding, also create geometric discontinuities that provide additional points of stress concentration. There are interesting possibilities in designing alloys that can reduce weld-induced residual stress through phase transformation. This was illustrated in a paper by Bhadeshia [6] who emphasised the important role that metallurgical phase transformations and associated shape changes play in affecting the development of residual stresses. He outlined the design of alloys such that the deformation caused by bainite and martensite transformations eliminates residual stress, leading to extraordinary improvements in the fatigue life of constrained structural assemblies. It is clearly highly beneficial to optimally design welding fabrication in terms of both process parameters, e.g. heat input, preheat and interpass temperatures, as well as in metallurgical terms through consideration of filler metal alloy content, cooling rate and post-weld heat treatment (PWHT).

Further complexity in life prediction arises from the modification of residual stress during cyclic loading and there is no definitive guidance available to assist with predicting this effect. A classic example of this aspect of stress modification during fatigue cycling is the relaxation of shot peening stresses in the fir tree root region of steam turbine blades during service, which could lead to blade failures in low pressure steam turbines. Other work reported by some of the present authors [7] details the work done in characterising residual stresses and fatigue life prediction for the last stage blades in the low pressure turbines of a 600 MW turbo-generator set. The residual stress field in the fir tree blade attachment region was measured on new unpeened and peened blades, and on ex-service blades using high energy synchrotron X-ray diffraction. Fig. 1 shows such a 23 kg last stage blade mounted on the stage of the ID15A instrument at the ESRF in France, for bi-axial measurements of the residual stress.

* Corresponding author at: School of Engineering, University of Plymouth, Plymouth, England, United Kingdom.
E-mail address: mjames@plymouth.ac.uk (M.N. James).

http://dx.doi.org/10.1016/j.tafmec.2017.03.008
0167-8442/

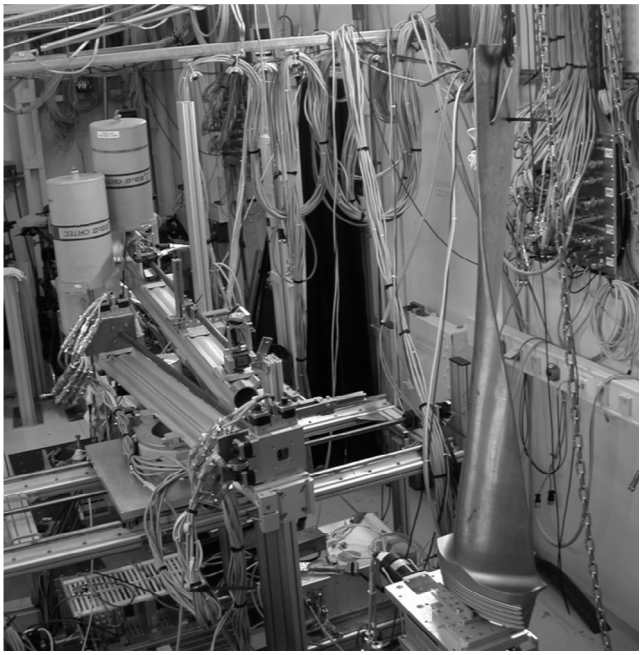

Fig. 1. Bi-axial measurement of residual stresses in a 23 kg 12CrNiMo martensitic steel turbine blade.

Shot peening has been used for many years as a means of combatting fatigue failure via mechanical pre-stressing of the surface of engineering parts; Cary [8] and Guagliano [9] have both provided interesting reviews of its chronological development. Tensile residual stresses are usually the most detrimental in general service, and, in the presence of a macroscopic notch, they can also lead to fatigue crack initiation and growth during compression-compression fatigue. In these cases, the notch root region undergoes plastic deformation during the compressive part of the fatigue loading and develops a tensile residual stress field during the unloading part of the fatigue cycle. The superimposed compression fatigue loading then leads to tensile fatigue cycling in the cyclic plastic zone. An example of a situation where tensile residual stress associated with compression fatigue of a notch can lead to fatigue crack growth is that of hard materials [10], where the phenomenon can be useful in pre-cracking of standard fracture toughness specimens, e.g. [11]. Fatigue crack growth under compression-compression loading has been analysed by Vasudevan and Sadananda [12] while Lenets has considered environmentally-assisted compression fatigue of metallic materials [13]. Examples of this mechanism in action, leading to failure of aircraft landing gear struts and other components, have been reported [14].

Predicting fatigue performance in the presence of residual stress fields remains complex, particularly for welded structures, although documents such as BS 7910:2013 [12] now provide generalized guidance on residual stress profiles in as-welded joints (annex Q) and on the likely values of residual stress in structures subject to post-weld heat treatment (see Section 7.1.8.3) in an enclosed furnace with temperature ranges between 550 °C and 620 °C. The guidance further notes, however, that where local post-weld heat treatment is carried out no general recommendations can be given and conservative assumptions should be made; this would be the usual case for any large structure that contains welds (either from fabrication or from repair processes). Stacey et al. [15] have discussed the incorporation of residual stress assessment procedures into the EU SINTAP defect assessment procedure and note that the SINTAP procedure is built on the guidance contained in BS 7910 and the CEGB R6 procedures. SINTAP is an acronym for Structural Integrity Assessment Procedures, a project funded by the European Community whose aim was to develop a unified procedure for European Industry that covered structural integrity assessment of structures and components.

It is the premise of this paper that accurate life prediction relies on detailed experimental assessment of residual stresses, often combined with simulation using numerical analysis techniques, e.g. Ref. [7]. In recent years, very significant advances have been made in the ability to perform full-field measurements of residual stresses via sophisticated 3D synchrotron X-ray and neutron diffraction techniques, using automated stages that allow precise location of measurement points, coupled with software-driven data analysis. At certain facilities, including the Institut Laue-Langevin (ILL) and the European Synchrotron Radiation Facility (ESRF) in Grenoble, France, it is also possible to apply fatigue loading in-situ on a beamline whilst making residual stress measurements. For critical engineering applications, 3D residual stresses can then be measured at points of local stress concentration and used to calibrate detailed finite element models of complex welded (or other) structures, and hence to produce estimates of fatigue life under the loading conditions of interest. These nondestructive techniques along with other destructive techniques for measuring residual stress are outlined by Withers [1] in a review paper.

It can be posited that structural life prediction under cyclic loading is probabilistic in nature, at least in part, because each weld in a structure comprises an individual ‘system’ whose behaviour is influenced by material, metallurgy, loading, environment, manufacture and fabrication. A significant part of this variation arises from the differences in residual stresses that exist between nominally similar welds and structural geometries (or even rolled members), resulting from relatively minor variations in these factors. Thus structural life prediction essentially deals with the analysis of a ‘system of systems’ and further advances in accuracy of life prediction, or in the treatment of residual stress issues, may require the incorporation of new systems analysis tools into our prediction methodologies. The analysis of ‘systems of systems’ is an emerging discipline and the methodology for defining, abstracting, modelling, and analysing ‘system of systems’ problems is still incomplete. Nonetheless, as we move towards ‘smart’ structures with embedded sensors for condition monitoring, concepts relevant to the analysis of ‘systems of systems’ and networks of ‘things’ (which is one type of distributed system) are likely to become more relevant to life prediction for complex structures. Work is currently ongoing to define the characteristics of ‘systems of systems’ and a very interesting discussion on the concept of the Network of ‘Things’ is provided by Voas in a free US National Institute of Standards and Technology document [16]. The document sets out, in the context of “systems with large amounts of data, scalability concerns, heterogeneity concerns, temporal concerns, and elements of unknown pedigree with possible nefarious intent” the underlying foundation science to explore the reliability and security of networks of ‘things’. Whilst not directly transferable to a structural ‘system of systems’ it points the way to new concepts in thinking about systems analysis, which is an integral part of the complexity involved in ensuring structural reliability.

Condition monitoring in service is required as an integral part of a fracture mechanics-based life assessment for complex structures that supports run-repair-replace decisions. In thermal power generation, there are stringent requirements stipulated for repair processes on, for example, boilers, pipework and pressure vessels. Part of the certification procedure for new repair techniques and their incorporation into codes and standards involves an assessment of the residual stresses induced during repair and their potential alleviation through post-weld heat treatment (PWHT). The overall intention in the repair process is to deliver the component back

into service in a state as near as possible to the one that it had on original service entry.

The emergence in recent years of solid state friction processing techniques offers new opportunities to reduce the cost of repair for certain classes of power generation problems and to concomitantly lower peak values of residual stress. Amenable problem areas include cost-effective assessment and repair of creep damage or localised cracking for thermal power plant pipework, and cracks and other defects in turbine rotor disc and blade attachment holes, e.g. [17]. The following paper, which is an extended and modified version of [18], is intended to summarise some recent work by the authors in the two linked areas of innovative application of friction processing to thermal power plant components and detailed measurement of the weld-induced residual stress that then forms a part of the assessment of the fatigue and fracture performance, and hence assists in combatting failure during subsequent service. It therefore presents data that has previously been published as well as discussing new results from neutron diffraction measurements of residual stress.

2. Weld repair in power generation components

2.1. Assessment and repair of steam turbine blade attachment slots

Turbine failures resulting from blade and rotor disc problems cost the power generation industry substantial annual amounts of money [17]. Alongside a desire to reduce these costs, there are strong additional economic pressures to move towards sample-based condition monitoring and a probabilistic fracture mechanics-based life assessment. It is therefore clear that more cost-effective techniques for assessment of creep damage and cracking, where the sampling procedure and repair process are integrated into a single operational platform, would be very attractive to power station operators. Hattingh et al. in Ref. [17] discussed the deployment of an innovative bespoke friction taper hydro-pillar (FTHP) welding technique to repair stress corrosion cracks (SCC) in the central blade attachment prong of a last stage LP turbine disc in a 200 MW unit. The unique FTHP platform (see diagram in Fig. 2) developed for this application has a modular design which enables site applications in various orientations and configurations. One such application required that the device be mounted on a high pressure (HP) steam turbine rotor and then performing a sequence of operations that included extracting annular samples from the highly stressed and inaccessible corner radius of the blade attachment T-slot for creep analysis, before repairing the hole by FTHP welding. This was followed by re-machining of the T-slot and heat treatment of the welded area.

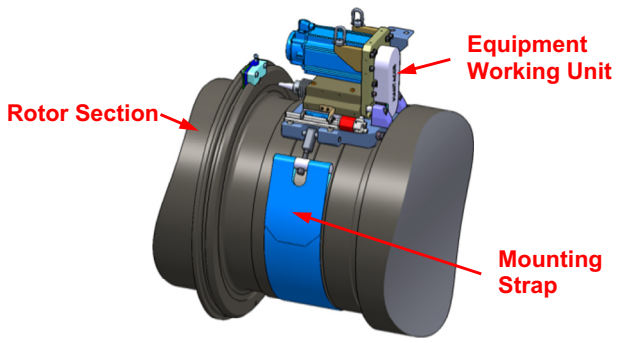

Fig. 2. Illustration of the bespoke FTHP platform in position on a stream turbine rotor. It uses the registered WeldCore® process and is capable of extracting an annular metallurgical sample through the thickness of the blade attachment T-slot wall, repairing and re-drilling the hole in a single sequence of operations.

The technique employs the so-called WeldCore® process and the FTHP welding process, that is now accepted by ASME for inclusion as a new welding process in Section IX of their Boiler and Pressure Vessel Code [19].

An integral part of the certification of a new repair technique involves the assessment of residual stresses and, in work that underpinned deployment of the FTHP process, residual stresses were measured in five specimens of low pressure steam turbine steel conforming to the German specification SEW 555 Grade 26NiCrMoV1-5 (ASTM A470 Class 5–7) representing the various stages in the repair process (see Fig. 3). This work was performed at the ILL in Grenoble, France, in experiment 1-02-83 using the SALSA beamline. In this case, knowledge of the residual stresses was important in assessing the effectiveness of PWHT in reducing peak residual stress values to <100 MPa. The stresses during service (applied plus residual) would then be approaching those applicable to the original blade root attachment hole and the turbine could continue in operation with the operator anticipating a similar fatigue/SCC performance to the original blade, provided that significant weld defects are not present. When performed using optimum process parameters, FTHP leads to a defect population that is less numerous and generally smaller in size than that found with fusion processes. The PWHT involved heating the specimens (each 95 mm × 95 mm × 18 mm) in a furnace at 680 °C for 1 h followed by furnace cooling. Although the temperature of 680 °C is above the typical manufacturing tempering range of 630–650 °C, it is still sufficiently below the A_{C1} temperature for this steel (typically ranging from 750 to 780 °C; A_{C1} is the austenite transformation start temperature on heating the steel) and the PWHT was therefore intended to achieve maximum stress-relaxation by reducing the yield strength of the material to the level of an acceptable residual stress (<100 MPa). The effectiveness of PWHT is illustrated in Fig. 4, which shows the Vickers microhardness profile at three depths in the 18 mm thick W5 specimen (undrilled with PWHT); it is clear that they have been substantially reduced from the peak values of ~500 H_V observed with the as-welded and undrilled specimen (W2). Note that the coordinate axes are defined as x and z transverse to the hole and y is defined through the thickness with zero at the upper surface of the specimen. Fig. 5 compares the residual stress at three depths in specimen W2 with W5; peak magnitudes are reduced from circa 400 MPa to 500 MPa to <100 MPa. The results also indicated that drilling an 8 mm hole in the as-welded specimen (W3), to simulate a new pin attachment hole, led to a positive residual stress near the free surface in the x and y-coordinate directions; PWHT (W4) then decreased the magnitude of the residual stress around the hole to <100 MPa in all three coordinate directions [17].

2.2. Damage assessment and repair of thick-walled steam pipe

Janovec et al. [20] discussed the assessment of creep damage and life assessment for BS EN10216 Grade 14MoV6-3 (Material number 1.7715) steam pipes in Czech power plants. They stated that in terms of destructive assessment of through-thickness creep damage "it is necessary to interrupt the operation and remove a part of the steam pipeline". This is clearly a very costly way of sampling through-thickness information on creep damage that is not available from either surface replication or 'boat' sampling techniques [21]. However, the FTHP process is not restricted to repairing damage at turbine blade attachment slots on LP turbines and can also be used for in-situ through-thickness creep specimen sampling in thick-walled steam pipe.

In this respect, the present authors have performed trial creep sampling work on 750 mm long sections of thick-walled (42 mm) steam pipe with an outer diameter of 366 mm, manufactured from Grade 1.7715 steel. The work used the WeldCore® technique

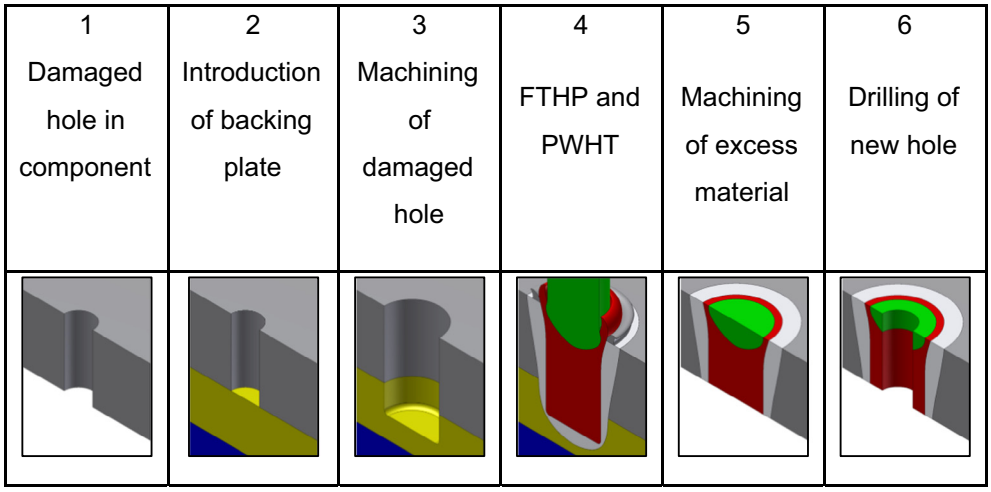

Fig. 3a. Stages in the FTHP repair of damaged turbine blade attachment finger holes in a LP rotor disc. Residual stress measurements were made on specimens representing stages 5 and 6 in both the as-welded and PWHT conditions.

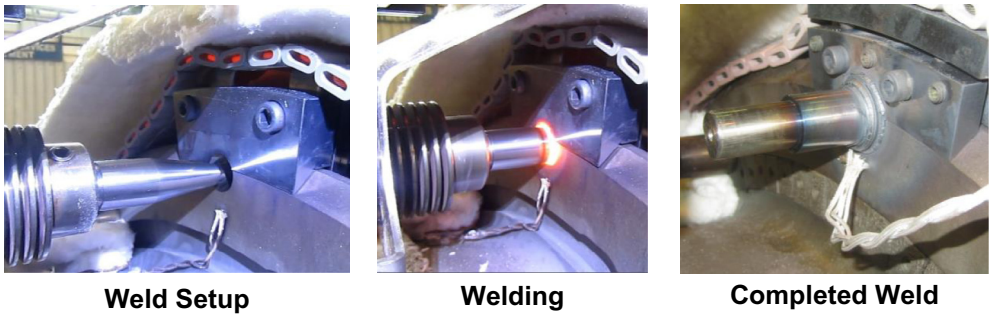

Fig. 3b. Images showing the welding stages in the FTHP process.

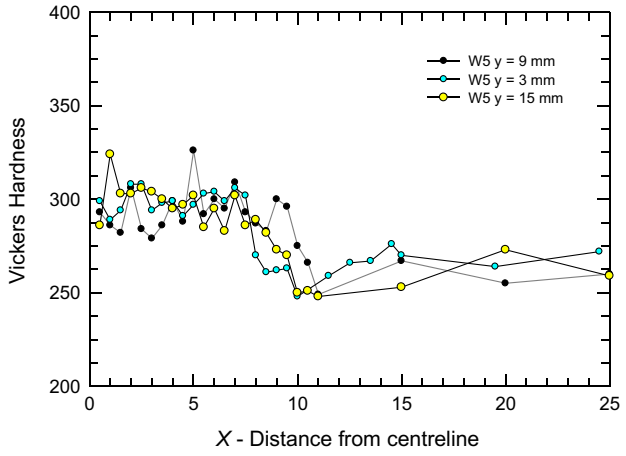

Fig. 4. Vickers hardness profiles under a 500 gf load in specimen W5 (un-drilled and PWHT) at three depths in the 18 mm thick steel.

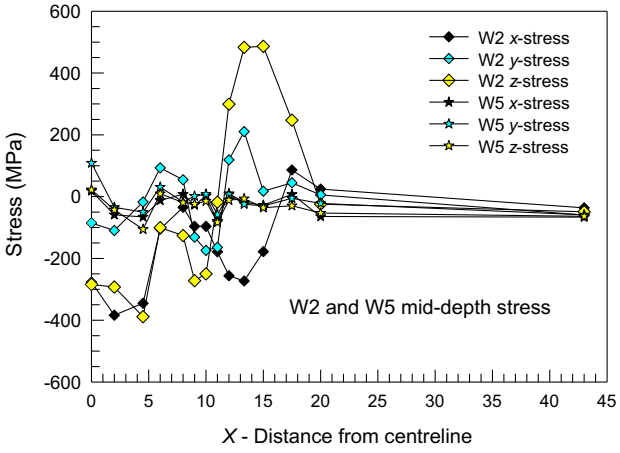

Fig. 5. Comparison between the mid-depth values of residual stress in all three coordinate directions for specimens W2 (as-welded and undrilled) and W5. The edge of the original hole in the blade would have been at the x = 4 mm position.

and a similar bespoke FTHP processing platform similar to that discussed above. Grade 1.7715 is a Cr-Mo-V (Cr 0.30–0.60; Mo 0.50–0.70; V 0.22–0.32) alloy steel used to manufacture seamless pipe for high temperature and pressure service. It typically has a tensile strength R_m in the range 460–610 MPa and a minimum yield strength R_{eH} in the range 300–320 MPa. In Experiment 1-02-128 performed on the SALSA beamline at the ILL in Grenoble, the residual stresses were measured in specimens cut from these sections of steam pipe. The aim in this experiment was again to determine the effectiveness of PWHT, in this case using localized induction heating of the steel pipe, after creep sample removal and integrated repair welding. High levels of tensile residual stress in the sampling region would be detrimental to the remaining lifetime of the component.

The sequence of events in the WeldCore® creep sampling process is shown in Fig. 6. In the original planning for this experiment,

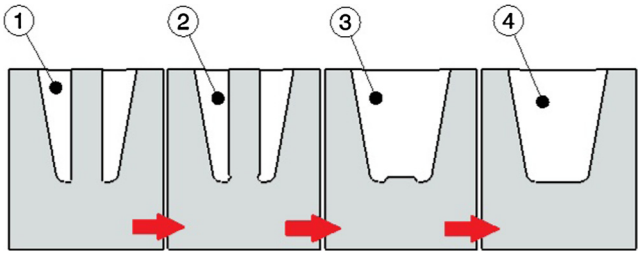

Fig. 6a. Sequence of events that occur in the WeldCore® process using a bespoke FTHP processing platform. Stage 1 delivers a cored hole; stage 2 undercuts the core, stage 3 is after core removal and stage 4 represents a hole prepared for repair.

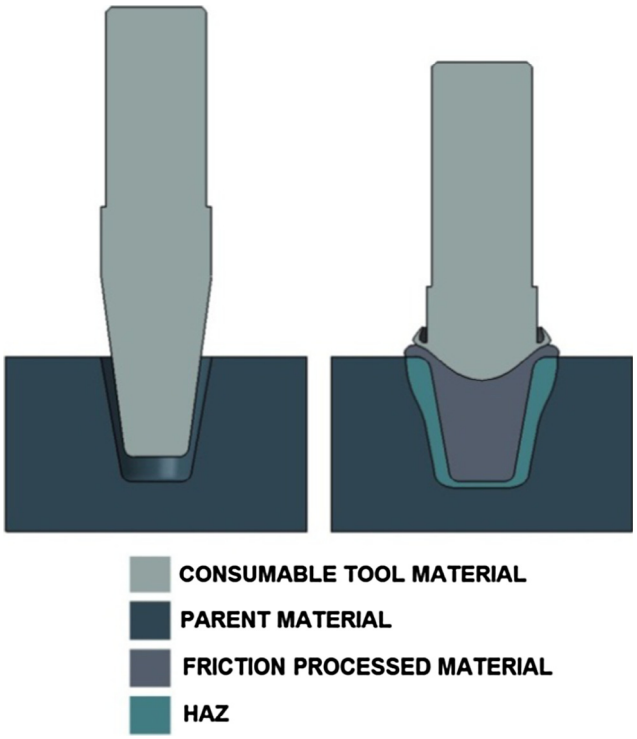

Fig. 6b. This diagram represents the final stage in the WeldCore® process where the prepared hole is filled by friction taper hydro-pillar processing (FTHP).

specimens were prepared from two locations spaced at 90° intervals around the circumference of the pipe. At each position one as-welded specimen and one specimen that had been subjected to localised post-weld induction heat treatment were prepared. However, in the beamtime available in Experiment 1-02-128 it became necessary to concentrate the residual stress measurement effort on a single as-welded specimen (1A) and on a single specimen (2B) that had been welded and subjected to in-situ PWHT by induction heating. Fig. 7 illustrates the PWHT of the pipe specimen using an induction heating coil and a thermally insulating pad. The specimens 1A and 2B were cut from circumferential positions 90° apart and a direct point-based comparison between the residual stresses before and after PWHT is therefore not possible. This highlights the point that in real life structural engineering, even when using advanced neutron diffraction strain scanning instruments, it is difficult to obtain sufficient access to beamtime to perform all the necessary experiments to underpin the industrial adoption of new techniques and processes.

Nonetheless the residual stresses in the pipe would be expected to be similar at the two circumferential positions. Full details of the FTHP process are given in Table 1 and the consumable tool was

Fig. 7. Induction heat treatment of the pipe after completion of the WeldCore® process.

manufactured from BS EN 10216 Grade 10CrMo9-10 (Material number 1.7380). The PWHT was limited to a maximum surface temperature of 800 °C and induction heating was continued until the inner surface of the pipe reached 650 °C which was then maintained for a minimum of 15 min. Cooling took place in still air conditions in the laboratory.

Measurements were made of the residual stresses in the hoop, radial and axial directions of the pipe at three positions through the wall thickness (18 mm, 27 mm and 37 mm from the outer surface) at a number of positions from the weld centreline to a distance of 60 mm. Fig. 8 shows the measured residual hoop stresses in specimen 1A (as-welded – Fig. 8a) and specimen 2B (PWHT – Fig. 8b) while Fig. 9 shows the corresponding data in the axial direction. In terms of crack initiation during service, these are the two key coordinate directions. Measurements were able to be made at 5 depths in the PWHT specimen, while data was obtained at only three depths in the as-welded specimen.

Certain observations can be made from these hoop stress data; firstly, that at depths of 18 mm, 27 mm and 37 mm below the surface of the pipe, the large negative peaks that occur around the edge of the weld metal are reduced from peak values in the range 380–450 MPa in the as-welded state, to values after PWHT in a range around 275–380 MPa. Secondly, the values of peak tensile hoop stress are also reduced at equivalent depths and, thirdly, the stress distribution moves in the tensile direction the closer to the outer surface the measurements are made (e.g. Fig. 9b, x = 9 mm and x = 4 mm). In all cases where data was obtained, the level of peak tensile residual hoop stress is <120 MPa.

The same general observations are true of the axial stress measurements, although there is a significant difference in that the PWHT appears to sharply increase the stress variation across the heat-affected zone (HAZ) of the weld, between distances of 9 mm and 20 mm from the weld centreline. Peak values of tensile axial stress in all cases are <140 MPa. Although experimental difficulties led to a smaller set of residual stress measurements than originally planned, it is clear that the FTHP technique can be usefully employed for in-situ through-thickness creep sampling and that the level of tensile residual stress in the pipe wall is <50% of the lower yield strength of the steel. Localised PWHT reduces the peak negative stresses by some 16% in the hoop direction in the pipe and by up to 38% in the axial direction. A number of different in-situ applications of the FTHP technique have so far been successfully completed within the power generation and petrochemical industrial sectors.

Table 1
Details of the FTHP process.

Pin taper	Pin length (mm)	Pin end (mm)	Tool speed (rpm)	Forging force (kN)	Forging time (s)
15°	47.5	9	5000	27	20

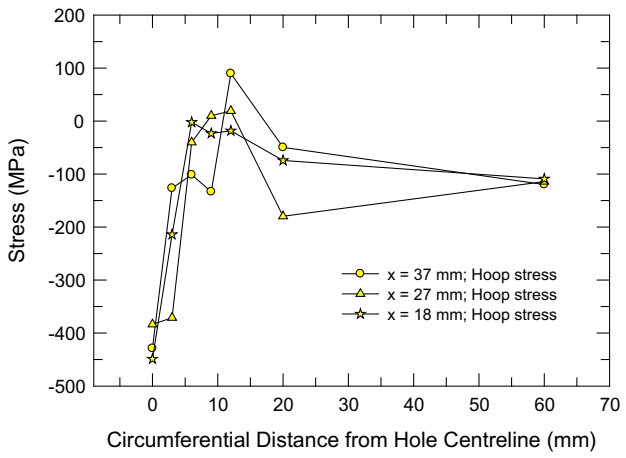

Fig. 8a. Residual hoop stresses in the as-welded FTHP specimen 1A.

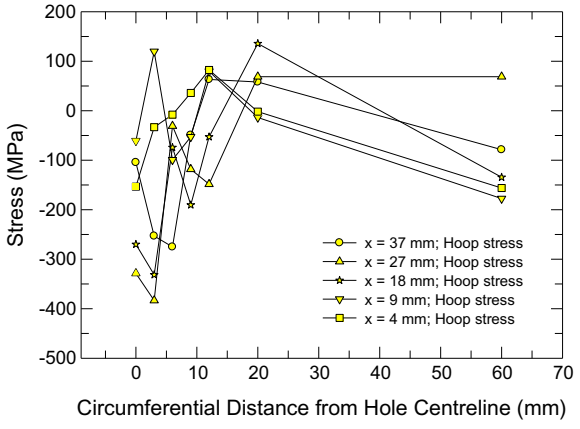

Fig. 8b. Residual hoop stresses in specimen 2B after local PWHT by inductive coil.

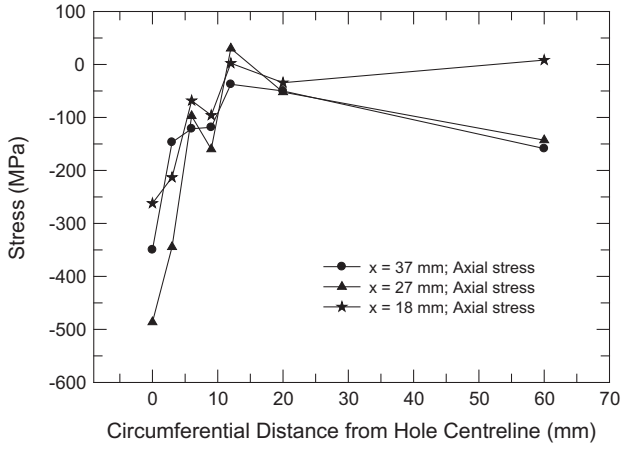

Fig. 9a. Residual axial stresses in the as-welded FTHP specimen 1A.

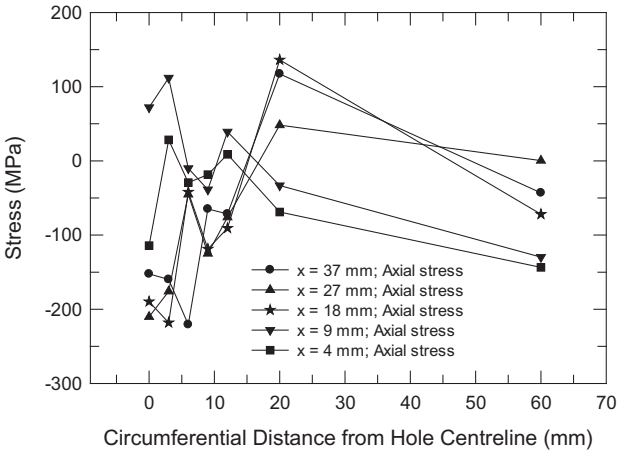

Fig. 9b. Residual axial stresses in specimen 2B after local PWHT by inductive coil.

2.3. Residual stresses in turbine blade shroud tenons after weld build-up

Tenons on turbine blades are used to position and fix the tips of adjacent blades in a shroud, whose function is to control the in-service vibration response of the blades. During turbine maintenance a large number of turbine blades have to be scrapped when their tenons are ground down in order to remove the blades for inspection or other maintenance activities. Typically, the estimated replacement cost of a row of blades is €60,000; and although in some cases only single blades have to be replaced, this still requires a number of adjacent blades to be scrapped in order to access and replace the damaged blade. Blades removed from the disc cannot be re-used as the remaining tenon stub is too short to be riveted to the shroud a second time. Fig. 10 shows a typical blade tenon configuration and illustrates the problem that arises from tenon grinding to remove the shroud.

Rebuilding tenons by welding is a viable option to refurbish the blades for further use and there is a strong incentive to implement this procedure in routine maintenance. However, tenons are subjected to high centrifugal loading during normal service operation at 3000 rpm and it is well known that the main blade failure mechanisms are SCC, hydrogen-assisted cracking or fatigue; failure modes that are all rendered more likely by high levels of tensile residual stress. These turbine blades are typically manufactured from a martensitic stainless steel such as EN 10269 Grade X12CrNiMoV12-3 (trade names FV566 or Jethete M152), whose nominal composition is 0.1C, 0.7Mn, 12Cr, 2.5Ni, 1.75Mo, 0.35V, 0.03N Mechanical properties were measured as 0.2% proof stress of 868 MPa and tensile strength of 1048 MPa. The alloy is known to be prone to stress corrosion and hydrogen-induced cracking when subjected to high localised stresses in a susceptible environment. It is therefore important to assess the level of weld residual stresses introduced by candidate weld repair processes, as an integral part of the risk assessment and certification procedure of the refurbishment technique. The aim of this work was to establish the magnitude of residual stress present in a low pressure steam turbine blade following build-up of the tenon by TIG and laser beam welding processes.

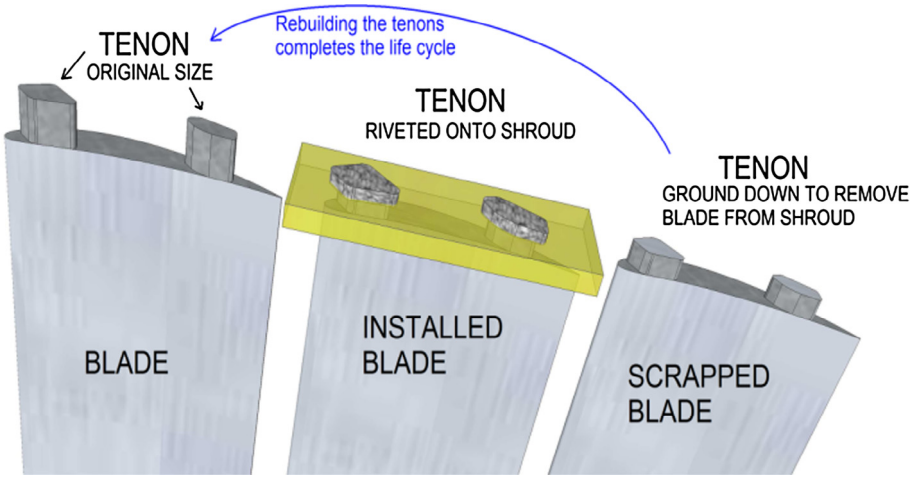

Fig. 10. Schematic illustration of the tenon rebuild issue.

Residual stress data were measured on the SALSA beamline at the ILL, Grenoble in Experiment 1-02-152 for simulated blade specimens in the as-welded and PWHT conditions for both welding processes. Neutron diffraction measurements were made using a collimated beam (λ = 1.644 Å) and cadmium shielding of the samples, resulting in a gauge volume of 0.6 × 0.6 × 12 mm. The 0.6 mm dimension was required for fine spatial resolution across the heat affected zone. The specimen geometry used to simulate the built-up, un-machined tenon is shown in Fig. 11 and takes the form of rectangular coupons 60 mm × 50 mm × 15 mm machined from ex-service Grade FV566 martensitic stainless steel turbine blades. Laser welding was performed at the National Laser Centre of the CSIR, South Africa, using a 3 kW IPG YLS-3000-TR power source with the welding head integrated with a KUKA KR60L30 robotic system positioner.

The full experimental matrix is shown in Table 2 and involved weld build-up using either an austenitic Nickel-based powder (type Inconel 625) or Grade FV520 martensitic stainless steel powder whilst maintaining a preheat of 200 °C. In this paper, we present the residual stress data obtained from specimens 1 and 2 (laser welding), and 4 and 5 (TIG welding) where the weld consumable used in the repair process was Grade FV520 martensitic stainless steel powder. In the laser welding case, the weld build-up was applied in 0.4 mm layers with beads 2 mm wide and 1 mm 'step-over' between beads with a heat input of 50.9 kJ/mm.

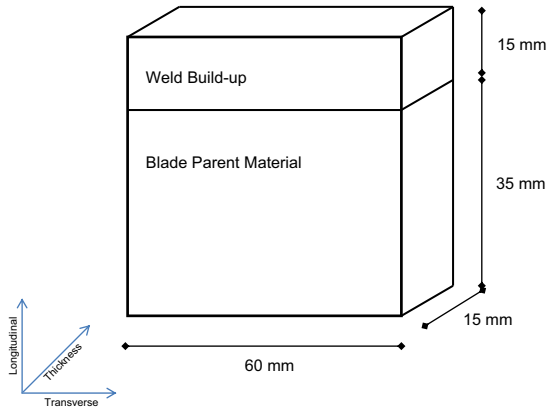

Fig. 11. Geometry of the DIN 1.4939 steel coupon used to simulate tenon build-up by laser welding. The three orthogonal directions for residual stress measurement are longitudinal (L), transverse (T) and short-transverse or through-thickness (ST).

Table 2
Grade FV520B martensitic stainless steel turbine blade specimens used for residual stress measurements in experiment 1-02-152.

ID number	Weld type	Condition
1	Laser weld - Martensitic consumable	As welded
2	Laser weld - Martensitic consumable	PWHT
4	TIG weld - Martensitic consumable	PWHT
5	TIG weld - Martensitic consumable	As welded
6	Laser weld - Austenitic consumable	As welded
7	Laser weld - Austenitic consumable	PWHT

The interpass temperature was maintained at 154 °C and the shielding gas was argon. PWHT involved heating at 100 °C/h up to 650 °C, holding this temperature for an hour then cooling at 100 °C/h.

For comparison a set of samples were prepared by automated TIG welding with a preheat of 100 °C and a maximum interpass temperature of 250 °C with a heat input of 0.5768 kJ/mm and a travel speed of 95.25 mm/min. The 1.2 mm diameter filler wire was a martensitic stainless steel with a nominal composition of 0.2C, 17Cr, 1.1Mo and 0.4Ni. The electrode oscillated perpendicular to the direction of travel with an amplitude of 6.35 mm, giving weld beads 12 mm wide and 2.5–3.0 mm thick. Total depth of weld build-up was 22 mm.

Residual stress data was measured in three orthogonal directions at an array of points down the centreline (in both the T and ST directions) of the simulated tenon repair specimens. In this tenon experiment (1-02-152) and in the blade attachment hole experiment (1-02-83), the unstrained lattice spacing d_0 was measured using toothcomb specimens electrodischarge machined (EDM) from the same material as the residual stress specimens [22]. Data for d_0 is necessary when calculating strain from Bragg's law using changes in crystal lattice spacing, which have to referenced to the unstrained spacing. In determining values of d_0 it should be noted that small cubes are better than toothcomb specimens to measure the strain-free lattice spacing, unless allowance is made for the macro-stress along the tooth [23], which was done in these cases. In the case of experiment 1-02-128 (creep damage assessment) small cubes were produced by EDM and then used to make strain-free lattice spacing measurements. Values of the elastic constants used in the calculations were Poisson's ratio ν = 0.28 and the elastic modulus E = 212.7 GPa.

The as-welded condition was represented by specimens 2 (laser weld) and 5 (TIG weld) with specimens 1 (laser weld) and 4 (TIG weld) representing the PWHT tenon build-up case. The resulting

3D residual stress data are shown and compared for the two cases in Fig. 12a (as-welded) and Fig. 12b (PWHT). The zero point for the *x*-axis of Fig. 12 is the bottom surface of the test coupon, so the original fusion boundary is at $x = 35$ mm.

For the laser welded specimen in the as-welded condition, it is clear that a substantial level of triaxial tensile stress exists on either side of the fusion boundary with peak values of circa 600 MPa. Across the fusion boundary the peak stresses reduce in magnitude with the values in the T and ST directions tending to be negative, while the longitudinal stress remains tensile. The turbine blade tenons in an as-welded state would hence be exposed to a significant risk of experiencing SCC, hydrogen-assisted cracking or fatigue. In contrast after PWHT, the residual stress peaks are more localised around the fusion boundary transition and the peak tensile values are reduced to between 100 and 120 MPa. A small region (≈2 mm wide) of triaxial tension still remains associated with the fusion boundary zone. PWHT has therefore been quite successful in the laser welded case in reducing residual stress magnitudes and hence in reducing the possibility of crack initiation and growth during service.

The TIG welded specimens show rather different behaviour with tensile stresses occurring near the fusion boundary for the as-welded case only in the transverse direction and having peak values <200 MPa. Measured residual stress values are negative in the L and ST directions with peak values much greater (circa −400 MPa) than those observed with the laser welding (circa −100 MPa). For the PWHT TIG welded specimen the overall pattern of the residual stress field is similar to that observed for the laser welded case although peak negative values of stress are significantly higher in the TIG welded case at around −400 MPa than the values in the laser welded case (−300 MPa). The PWHT appears to primarily have affected residual stresses in the transverse direction and has made them more negative.

The heat input during welding is far lower for the laser process. This results in a narrower heat affected zone and significantly less distortion of the tenon build up. The difference between the as-welded condition residual stresses is largely due to the over-bead tempering effect during the TIG process. After PWHT the residual values are similar in amplitude, but the residual stresses in the TIG welded sample still dissipate further from the fusion zone.

Bendeich et al. [24] have reported neutron diffraction data measured on test coupons and on martensitic stainless steel low pressure steam turbine blades laser clad with Stellite 6, which is a cobalt-base high Cr wear resistant alloy. A cladding layer ~17 mm wide and ~1 mm thick was deposited on the tip section of the blades (~3–4 mm thick) and residual stresses were then measured on an as-welded blade and on a blade after PWHT at 625 °C for 2.5 h. Their gauge volume in these measurements was 1.0 mm × 1.0 mm × 5.0 mm and their results indicated that the PWHT was effective in reducing the stresses imparted by the laser cladding process with the small remaining stresses ascribed to differences in thermal expansion between the martensitic stainless steel blade and the Stellite cladding. These results support the observations made in the present work that PWHT at 650 °C is effective in relieving the tensile residual stresses that are induced during laser welding and in the present case PWHT also causes the laser welded region to be dominated by compressive residual stresses. Both of these factors would greatly reduce the possibility of crack initiation and growth under service loading.

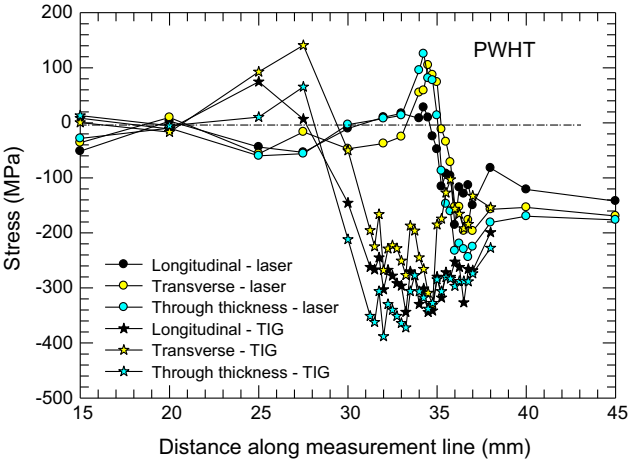

Fig. 12b. Residual stress data measured in the PWHT laser (specimen 1) and TIG welded (specimen 4) tenon samples.

It can be concluded from this experiment that laser welding refurbishment of the tenons on FV520 martensitic steam turbine blades, coupled with an appropriate PWHT process, offers a cost-effective way of repairing blades after shroud removal during turbine maintenance.

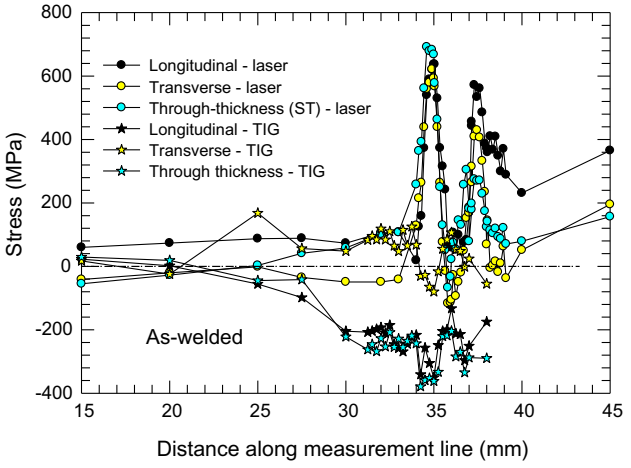

Fig. 12a. Residual stress data measured in the as-welded laser (specimen 2) and TIG welded (specimen 5) tenon samples.

3. Conclusions

This paper has presented examples drawn from the power generation industry, related to cost-effective damage assessment and repair of steam turbine components. Its purpose was to illustrate how detailed 3D measurements of residual stresses are an essential part of a structured approach to condition monitoring and to reducing the probability of fatigue and fracture, particularly in respect of certification of innovative new repair procedures. Advanced neutron and synchrotron X-ray diffraction facilities, such as those at the ILL and the ESRF in Grenoble, France offer a very significant capability in measuring 3D residual stress distributions in substantial pieces of engineering hardware (up to circa 500 kg mass) with 10 μm precision, relatively fast acquisition times and automated analysis of diffraction peaks. Such high resolution data can be coupled with finite element analysis to predict residual stress distributions in components and structures under different conditions and hence make predictions of fatigue life [7].

The main conclusion in the paper is that the innovative use of solid-state friction taper hydro-pillar processes can offer additional capability in condition monitoring of through-thickness creep damage in thermal power plant, as well as provide cost-effective local repair of creep or fatigue damage in, for example, thick-walled steam pipe and blade-disc attachment holes.

Creep assessment samples can be extracted up to about half the wall thickness, in-situ on thick-walled steam pipe. This provides a very significant improvement on current through-thickness techniques where a section would have to be cut from the pipe and a replacement piece fusion welded back into it. Solid-state friction processes lead to lower peak magnitudes of residual stress and local induction heat treatment can further reduce the level of residual stress, compared with fusion welding.

Acknowledgements

The award of beamtime on the SALSA instrument at the Institut Laue-Langevin, Grenoble through experiments 1-02-83, 1-02-128 and 1-02-152, together with the support of the beamline scientist, Dr. Thilo Pirling, are gratefully acknowledged.

References

[1] P.J. Withers, Residual stress and its role in failure, Rep. Prog. Phys. 70 (2007) 2211–2264.
[2] M.N. James, D.J. Hughes, Z. Chen, H. Lombard, D.G. Hattingh, D. Asquith, J.R. Yates, P.J. Webster, Residual stresses and fatigue performance, Eng. Fail. Anal. 14 (2007) 384–395.
[3] M.N. James, Residual stress influences on structural reliability, Eng. Fail. Anal. 18 (2011) 1909–1920.
[4] J. Hidveghy, J. NMichel, M. Bursak, Residual stress in microalloyed steel sheet, Metalurgija 42 (2003) 103–106.
[5] M. De Giorgi, Residual stress evolution in cold-rolled steels, Int. J. Fatigue 33 (2011) 507–512.
[6] H.K.D.H. Bhadeshia, Developments in martensitic and bainitic steels: role of the shape deformation, Mater. Sci. Eng., A 378 (2004) 34–39.
[7] M. Newby, M.N. James, D.G. Hattingh, Finite element modelling of residual stresses in shot-peened steam turbine blades, Fatigue Fract. Eng. Mater. Struct. 37 (2014) 707–716.
[8] P.E. Cary, History of shot peening, in: 1st International Conference on Shot Peening, Paris, France, 1981, pp. 23–28.
[9] M. Guagliano, Perspectives and problems in shot peening, a mechanical treatment to improve the fatigue behaviour of structural parts, Anales de Mecánica de la Fractura 28 (2011) 9–19.
[10] S. Suresh, The failure of hard materials in cyclic compression: theory, experiments and applications, Mater. Sci. Eng., A 105–106 (Part 2) (1988) 323–329.
[11] M.N. James, A.M. Human, S. Luyckx, Fracture toughness testing of hard metals using compression-compression precracking, J. Mater. Sci. 25 (1990) 4810–4814.
[12] A.K. Vasudevan, K. Sadananda, Analysis of fatigue crack growth under compression–compression loading, Int. J. Fatigue 23 (Supplement 1) (2001) 365–374.
[13] Y.N. Lenets, Compression fatigue crack growth behavior of metallic alloys: effect of environment, Eng. Fract. Mech. 57 (1997) 527–539.
[14] T.-Y.J. Hsu, Investigation of cyclic deformation and fatigue of polycrystalline Cu under pure compression cyclic loading conditions, in: PhD degree, Department of Materials Science, University of Toronto, Toronto, 2015, p. 198.
[15] A. Stacey, J.Y. Barthelemy, R.H. Leggatt, R.A. Ainsworth, Incorporation of residual stresses into the SINTAP defect assessment procedure, Eng. Fract. Mech. 67 (2000) 573–611.
[16] J.M. Voas, Networks of 'Things', in: NIST Special Publication 800–183, 2016.
[17] D.G. Hattingh, M.N. James, M. Newby, R. Scheepers, P. Doubell, Damage assessment and refurbishment of steam turbine blade/rotor attachment holes, Theoret. Appl. Fract. Mech. 83 (2016) 125–134.
[18] M.N. James, D.G. Hattingh, D. Asquith, M. Newby, P. Doubell, Applications of residual stress in combatting fatigue and fracture, Proc. Struct. Integrity 2 (2016) 11–25.
[19] ASME, ASME Boiler & Pressure Vessel Code Supplement 3, in: Section IX: Welding, Brazing and Fusing Qualifications, American Society of Mechanical Engineers, New York, USA, 2015.
[20] J. Janovec, D. Polachova, M. Junek, Lifetime assessment of a steam turbine, Acta Polytech. 52 (2012) 74–79.
[21] D.J. Gooch, 5.07 - Remnant Creep Life Prediction in Ferritic Materials A2 - Karihaloo, B., Milne, I. and Ritchie, R.O., in: Comprehensive Structural Integrity, Pergamon, Oxford, 2003, pp. 309–359.
[22] D.J. Hughes, M.N. James, D.G. Hattingh, P.J. Webster, The use of combs for evaluation of strain-free references for residual strain measurements by neutron and synchrotron X-ray diffraction, J. Neutron Res. 11 (2003) 289–293.
[23] S. Ganguly, L. Edwards, M.E. Fitzpatrick, Problems in using a comb sample as a stress-free reference for the determination of welding residual stress by diffraction, Mater. Sci. Eng., A 528 (2011) 1226–1232.
[24] P. Bendeich, N. Alam, M. Brandt, D. Carr, K. Short, R. Blevins, C. Curfs, O. Kirstein, G. Atkinson, T. Holden, R. Rogge, Residual stress measurements in laser clad repaired low pressure turbine blades for the power industry, Mater. Sci. Eng., A 437 (2006) 70–74.